EFFECT OF Ti AND N CONCENTRATIONS ON MICROSTRUCTURE AND MECHANICAL PROPERTIES OF MICROALLOYED HIGH STRENGTH LINEPIPE STEEL WELDS

Leigh Fletcher[1], Zhixiong Zhu[2], Muruganant Marimuthu[2], Lei Zheng[3], Mingzhuo Bai[3], Huijun Li[2] and Frank Barbaro[4]

[1]Welding and Pipeline Integrity; PO Box 413, Bright, Victoria, Australia
[2]Faculty of Engineering, University of Wollongong; Northfields Avenue, Wollongong, NSW, 2500, Australia
[3]Baoshan Iron & Steel Co., Ltd.; 899 Fujin Rd, Baoshan District, Shanghai, 201900, China
[4]Barbaro & Associates Pty Ltd, NSW, Australia

Abstract

A selection of nine heats of linepipe steel from the same project with different Ti and N content were used to evaluate the effects of Ti/N ratio on weld zone microstructure, hardness and prior austenite grain size (PAGS) in the coarse grained heat-affected zone (CGHAZ). It was shown that the microstructure of the base metal (BM) mainly consisted of fine grained polygonal ferrite with fine islands of pearlite. The weld metal (WM) microstructure was predominantly acicular ferrite with a small volume fraction of pro-eutectoid ferrite. The CGHAZ consisted of bainitic ferrite and islands of martensite-austenite (MA). The inside region of the pipe weld zone and base pipe was slightly harder due to the aging effects of the outer weld pass. The prior austenite grain size was shown to be consistent over the range of seam welding conditions and the range of Ti/N ratios was measured to be from 2 to 4.2.

Introduction

Over the last few decades, specifications of linepipe steels have moved from API 5L X52 to X70 and X80. This improvement in strength and toughness requires a corresponding improvement in the weld metal and heat-affected zone (HAZ). The coarse grained HAZ (CGHAZ) is a special focus of concern. The weldment experiences severe thermal cycles involving high temperatures and cooling rates [1]. Microstructural changes occur, for instance, precipitates coarsen and dissolve, and grain growth occurs within the HAZ surrounding the molten weld bead [2].

Grain size refinement is the only effective method for improving both strength and toughness. Steel production, alloy design and thermo-mechanical controlled processing are used to control grain size and microstructure and thus optimize mechanical properties and subsequent weld processing. A fine and homogeneous distribution of precipitates will contribute to grain size refinement when austenite transforms at low temperature. In welds, where high temperatures and cooling rates are involved, the kinetics of precipitation and grain growth vary significantly in contrast to cast or wrought structures. The presence of precipitates that do not dissolve or coarsen during the weld thermal cycle serve to limit the extent of grain coarsening in the heat-affected zone. The presence of TiN precipitates in the steel inhibits grain growth in the weld HAZ by

pinning the prior austenite grain boundaries. In improving the effectiveness of grain refinement an appropriate level of Ti and N concentrations in terms of their ratio has been identified as a good index [3, 4]. The density of the TiN particles needs to be sufficient to retard grain growth [4]. A high Ti content can decrease the pinning effect by formation of coarse TiN particles which also act as the initiation sites for cleavage fracture [5]. Beidokhti et al. report that Ti concentrations higher than 0.05% cause quasi-cleavage fracture due to formation of martensite-austenite (MA) micro-constituent [6]. Although there is no general agreement on the optimum Ti addition in high strength pipe steels, it is known that additions in excess of 0.06% are extremely detrimental to HAZ fracture toughness. It is thought that this is due to the formation of TiC at hyperstoichiometric values of Ti/N, and at high levels of Ti [7].

The optimal concentration of Ti and N is still the subject of debate for microalloyed steels. Bang et al. [8] showed by multiple regression analysis that the detrimental effect of free nitrogen was much greater than the beneficial effect of TiN on HAZ toughness. Doi et al. [9] showed that increasing Ti leads to an increase in the size of TiN precipitates which detrimentally affects the HAZ toughness. It has also been reported that the Ti/N ratio should be maintained lower than stoichiometric ratio of 3.42 to ensure a low coarsening rate of TiN inclusions [10]. But Wang's research [11] observed that the grain boundary pinning is most effective at the stoichiometric Ti/N ratio, i.e. 3.42 with TiN precipitates. Moreover, Chapa et al. [12] concluded through interpolation that the best Ti/N ratio for controlling austenite grain size would be close to 2.5. Medina [13] and Rak [14] also report that grain size control is optimised with a Ti/N ratio close to 2.

Research in Australia within the Energy Pipelines CRC (EPCRC) aims to provide a fundamental understanding of the effects of Ti and N contents on HAZ microstructures and properties. In the present paper a set of otherwise identical samples of API 5L grade X70 UOE pipe with a range of Ti/N ratio from 2.0 to 4.2 have been evaluated. The results are preliminary and are focused on the weld zone microstructure and hardness evaluation.

Experimental Procedures

Nine UOE pipe steel samples of API 5L X70 with varying Ti/N ratio were used for the study. All samples came from production pipe that exhibited good mechanical properties including weld metal and HAZ Charpy properties. In approximately 218,000 tonnes of pipe the HAZ Charpy values at -10 °C exceeded the minimum specified values, and the overall range was from 52 – 450 J. No correlation was found between Ti/N ratio and HAZ Charpy properties. The chemical compositions are shown in Table I. All these steels were welded using two-passes, one from inside the pipe and the other from outside, using submerged arc welding (SAW). The welding procedure and parameters are given in Table II. Heat input (HI) was calculated using the following equation:

$$HI = \mu \frac{60VI}{1000S}$$

where HI is heat input (kJ/mm), μ is welding process efficiency (0.95) [15–17], V is arc voltage (V), I is welding current (A) and S is welding travel speed (mm/min). Typical weld metal composition is shown in III.

Table I. Alloy Contents (wt. %) of 9 Pipeline Steels with Varying Ti, N Concentrations and Ti/N Ratios: The Base Composition of the Steel is Fe + - 0.25Si - 0.21Ni - 0.15Mo - 0.15Cu - 0.027V - 0.05Nb - 0.007P - 0.001S <3ppm B & 20ppm Ca

Sample No.	C	Mn	Al	Ti	N	Ti/N ratio
1	0.049	1.52	0.039	0.0093	0.0046	2.02
2	0.051	1.55	0.036	0.0081	0.0040	2.03
3	0.051	1.53	0.032	0.0084	0.0034	2.47
4	0.052	1.62	0.042	0.0100	0.0037	2.70
5	0.054	1.55	0.034	0.0084	0.0029	2.90
6	0.071	1.57	0.038	0.0110	0.0037	2.97
7	0.054	1.62	0.045	0.0110	0.0031	3.55
8	0.049	1.57	0.039	0.0088	0.0024	3.67
9	0.050	1.52	0.042	0.0093	0.0022	4.23
CE_{IIW}=0.36~0.40, P_{cm}=0.16-0.18.						

Table II. Submerged Arc Welding Parameters for Pipe Welds (3 Wire Process)

Welding Pass	Current (A)			Voltage (V)			Travel Speed (mm/min)	Heat Input (kJ/mm)
	1 (DC+)	2 (AC)	3 (AC)	1	2	3		
Inside	800	650	500	32	34	36	1600	2.34
Outside	900	600	500	34	38	40	1700	2.46

*Wire Classification: BHM-9; Stick out: 30±2 mm.

The UOE 14.1 mm thick pipes with diameter 1067 mm were sectioned and metallographically prepared for microstructural examination of the weld metal (WM), HAZ and base metal (BM).

All samples were etched with picric acid at 68 °C to obtain the austenite grain size in the CGHAZ. Grain size measurements were performed using the linear intercept method.

Table III. Average Weld Metal Composition for Both Inside & Outside Weld Deposited in Sample 2 in Table I: Fe + - 0.01P - 0.35Si - 0.0015S - 0.14Ni - 0.03Cr - 0.22Mo - 0.11Cu - 0.015Al - Ca < 0.0005wt%

	Outer Weld	Inner Weld
C	0.055	0.055
Mn	1.57	1.575
Mo	0.22	0.215
Nb	0.0295	0.031
Ti	0.0175	0.0165
V	0.0165	0.017
B	0.0011	0.0010

Metallography

A typical double submerged arc weld (DSAW) showing the critical regions of the HAZ is shown in Figure 1. Figure 2 shows the macrographs of the nine welds. The inner pass (bottom) is reheated by the outer pass (top). The weld shape and alignment was excellent and the contact angle at the weld toes was very good.

Austenite grain size varied around the fusion boundary of each weld and was related to weld shape and thermal cycle experienced locally. Maximum coarsening was observed under the shoulder/cap. Figure 3 shows the microstructure of the CGHAZ which is populated mostly with bainitic ferrite and aligned second phase assumed to be martensite-austenite (MA) islands. During the cooling process, the carbon atoms diffuse from the ferrite lath to the untransformed austenite. When the carbon concentration reaches a critical value and the carbon-rich austenite cools to a temperature below martensite start temperature (Ms), the remaining austenite partially transforms to martensite. This mixture of transformed martensite and untransformed austenite called MA constituent is commonly observed in the HAZ depending on the welding conditions. The size, distribution and aspect ratio of the MA constituent can affect the fracture toughness [18–20].
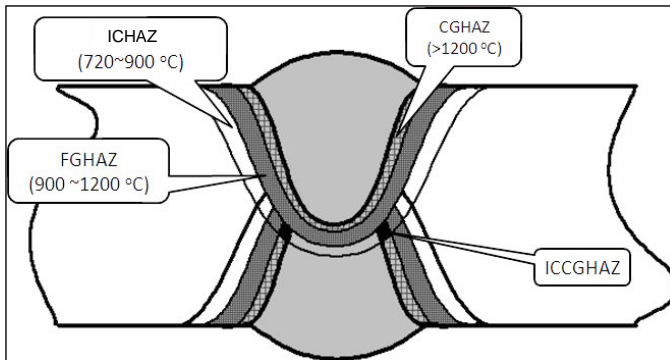
Figure 1. A double submerged arc weld showing: coarse grained HAZ (CGHAZ), fine grained HAZ (FGHAZ), intercritically heated HAZ (ICHAZ) and intercritically reheated CGHAZ (ICCGHAZ).
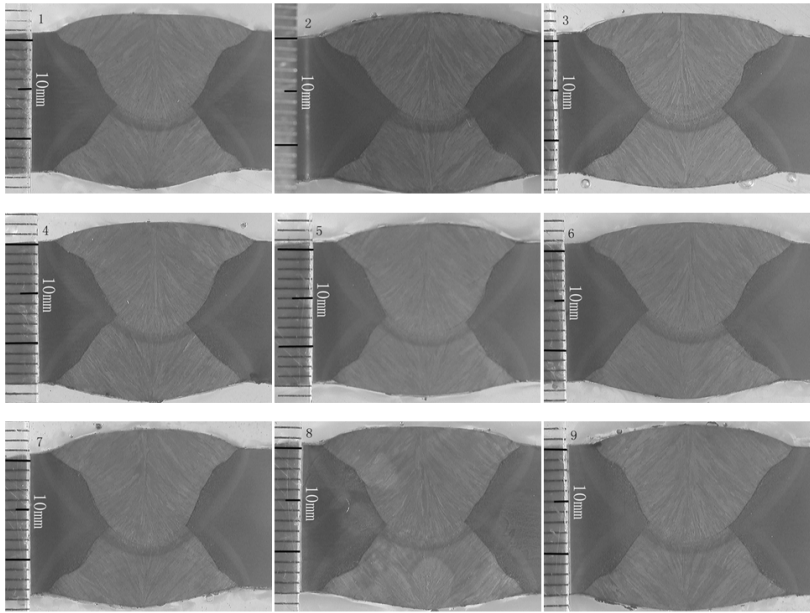
Figure 2. Macrographs of the welds showing the weldments from inside (bottom) and outside (top).

(a) Ti/N=2.02	(b) Ti/N=2.03	(c) Ti/N=2.47
(d) Ti/N=2.70	(e) Ti/N=2.90	(f) Ti/N=2.97
(g) Ti/N=3.55	(h) Ti/N=3.67	(i) Ti/N=4.23
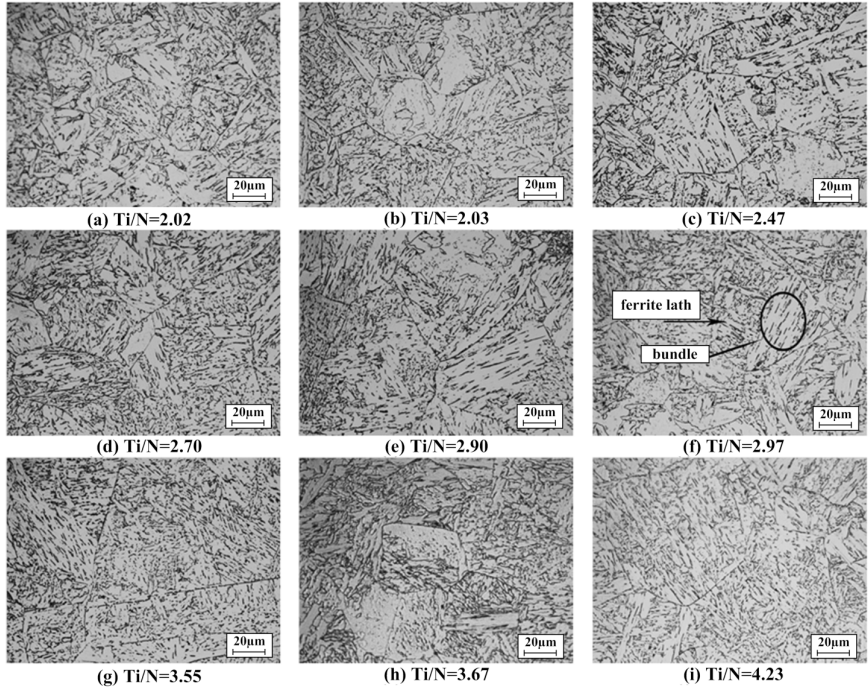
Figure 3. Optical micrographs of CGHAZ etched using 2% Nital at the point of inflection in the weld profile.

(a) Ti/N=2.02 **(b) Ti/N=2.03** **(c) Ti/N=2.47**

(d) Ti/N=2.70 **(e) Ti/N=2.90** **(f) Ti/N=2.97**

(g) Ti/N=3.55 **(h) Ti/N=3.67** **(i) Ti/N=4.23**
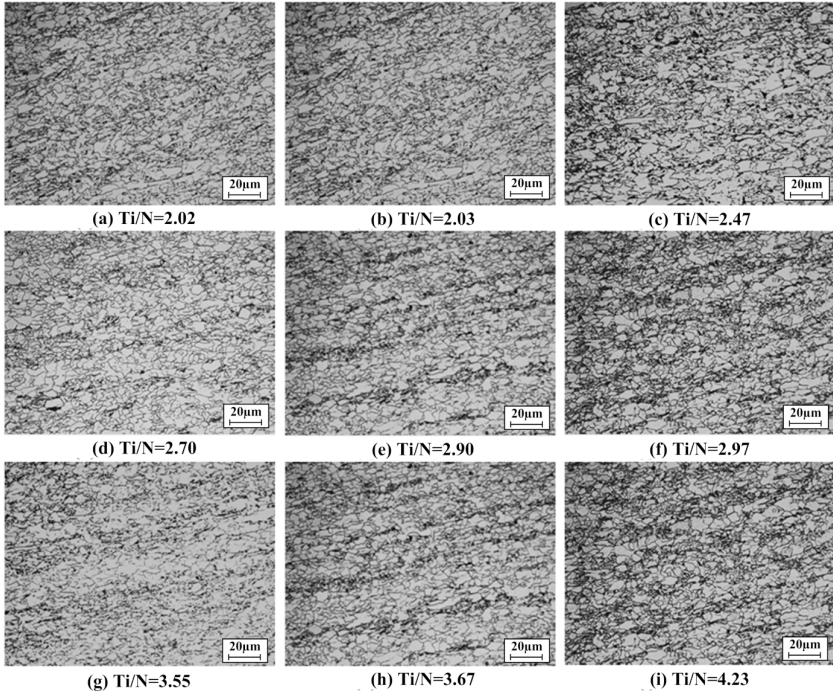
Figure 4. Optical micrographs of base metal etched using 2% Nital at quarter thickness location from top.
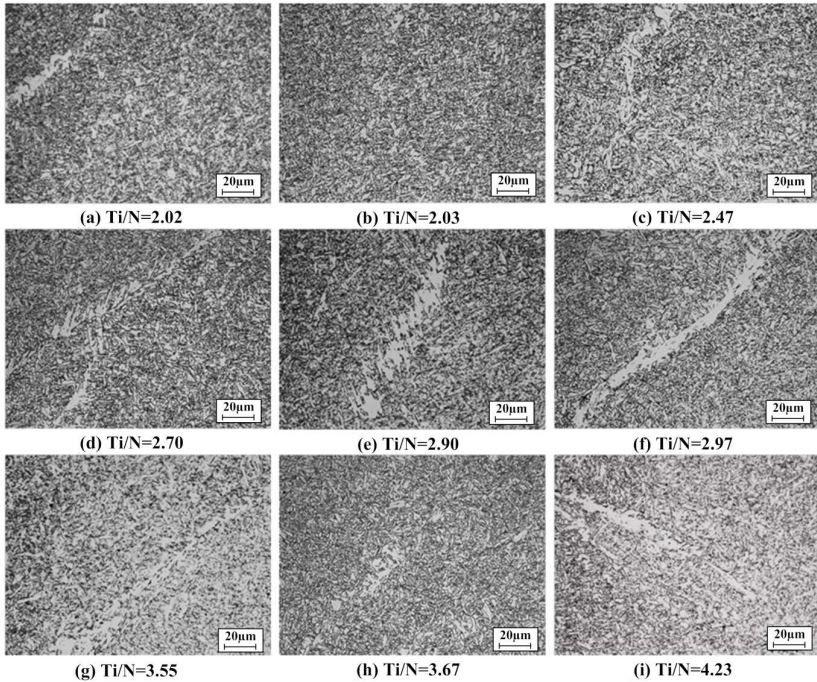
Figure 5. Optical micrographs of weld metal etched using 2% Nital in the central region of the external weld pass.

The microstructures of BM and WM are presented in Figure 4 & 5. As can be seen from Figure 4 the dominant microstructural constituent of the base metal was a very fine polygonal ferrite, although isolated patches of mixed grain size were observed. Fine islands of pearlite were also observed in the BM microstructure. The base metal also contained evidence of segregation in the mid thickness region of the plate.

Observation of weld metal micrographs shows the presence of pro-eutectoid ferrite and acicular ferrite as is typical of low alloy steel welds. It is well known that acicular ferrite in WM nucleates on and grows from non-metallic inclusions. Acicular ferrite is also known to provide an optimum combination of weld metal strength and toughness [21].

Grain Size

The prior austenite grain size measurements were performed close to the fusion boundary to capture the grain size variations in the CGHAZ. For the range of Ti and N evaluated the HAZ austenite grain size was well controlled and did not reveal any correlation with the Ti/N ratio, Figure 6.
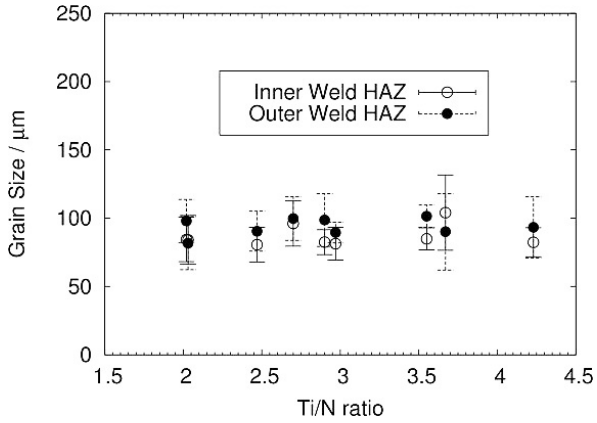
Figure 6. Austenite grain size measured along the weld fusion line at the CGHAZ.

Hardness

Hardness is an important indicator for the cold cracking resistance, strength, ductility, toughness and corrosion resistance [22]. Vickers hardness measurements were performed on the DSAW welds at the regions shown in Figure 7.
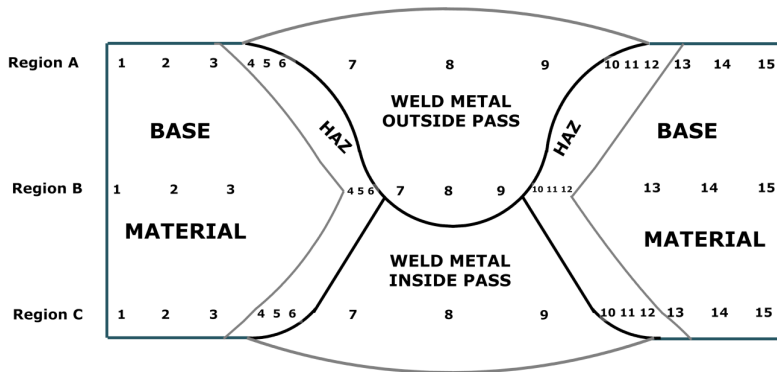
Figure 7. Schematic representation showing locations of Vickers hardness HV10.

Region A, B and C each had 15 indentations from left to right covering the base metal on both sides of the weld, HAZ and the weld metal. Microhardness indentations can be localized to phase constituents and can increase variability in results as defined by the indentation size effect (ISE) [23]. Hence, HV10 was employed to determine the average hardness of the microstructure.

Measured values of hardness for regions A, B and C are shown in Figure 8. The WM hardness overmatches the HAZ and BM.

No effect of Ti/N was found on the hardness values shown in Figure 8. A comparison of hardness in the three regions showed that the overall hardness of region C is higher than that of A & B. The fact that both weld deposits were produced under almost identical conditions (Table II) and possessed similar compositions (Table I) indicates the likelihood that the sequence of welding influenced the final hardness of the inside region of the seam weld and that the increase in hardness is due to precipitation hardening. As is shown in Figure 9 the internal weld HAZ also consistently exhibited a higher hardness.
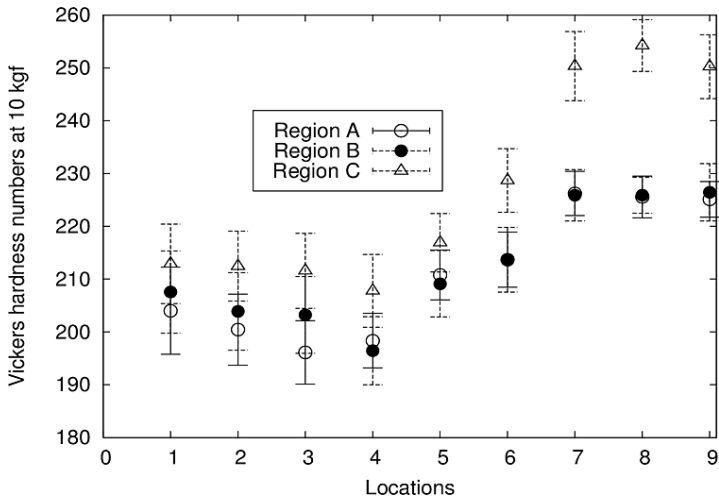
Figure 8. Vickers hardness of base metal, HAZ and fusion zone for the left hand locations shown in Figure 7. (The bars indicate the scatter in hardness as observed for the nine welds.)
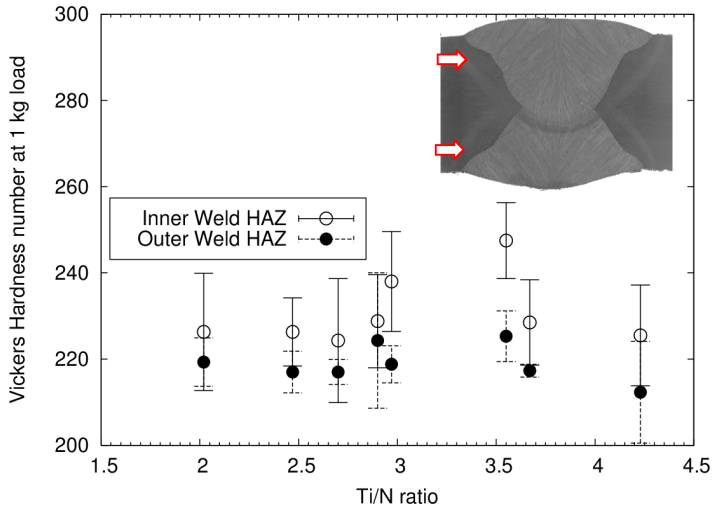
Figure 9. Hardness of HAZ for the internal (bottom) weld and the outer (top) weld. The size of the bars gives an indication of the lowest and the highest hardness observed in the respective HAZ.

Hardness Variation Down the Weld Centerline in DSAW Welds

Hardness measurements down the weld centerline revealed a marked difference in hardness of the outer (top) weld and the inner (bottom) weld, Figure 10. The hardness increase in the internal weld metal confirms the precipitation hardening effect.
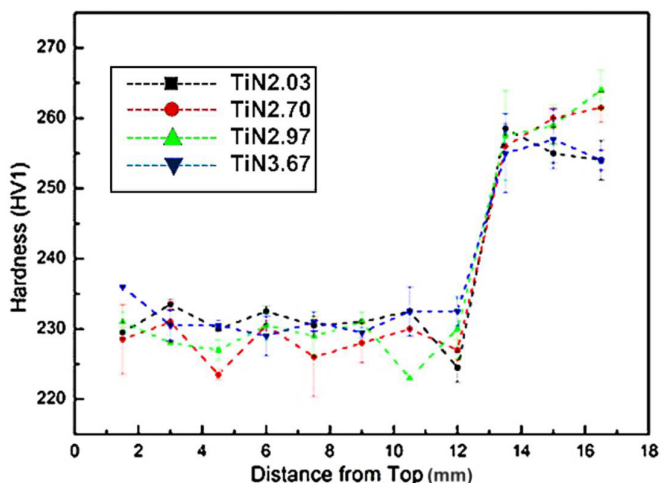
Figure 10. Weld metal centerline hardness at 1 kg load.

Aging Heat-Treatment

A heat treatment experiment on the base material has revealed the effect of aging. The hardness of samples heat-treated at 200, 400 and 600 °C for 2 min shown in Figure 11, revealed an increase in hardness at 400 °C subsequently decreasing at 600 °C. This increase can only be attributed to the age hardening phenomena associated with the presence of the microalloying elements, Ti, V and Nb. Further treating the samples at a higher temperature only over-ages and coarsens the precipitates thereby showing a dip in the room temperature hardness [24].

It is worthy to note that an overall increase in hardness is observed for the sample with a Ti/N ratio of 3.55 (Figure 11). This may be related to the complex interaction of the different microalloying elements with both carbon and nitrogen and will be part of the ongoing investigation within this research program of the Energy Pipelines CRC.
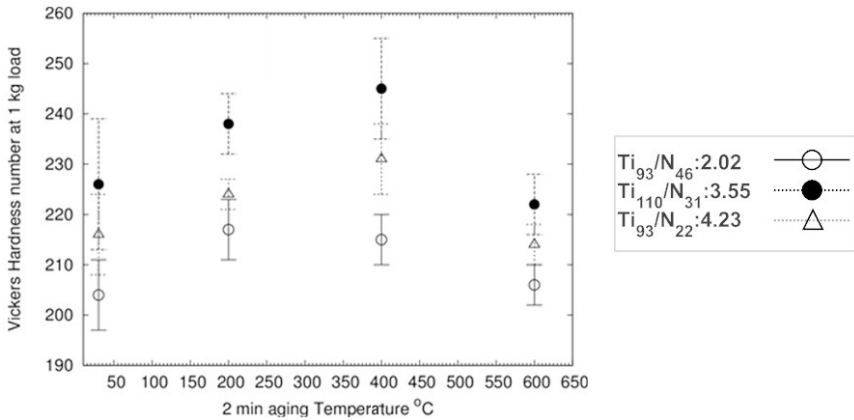
Figure 11. Hardness as a function of temperature and Ti/N ratio. Subscripts in the legend refer to ppm of the respective element.

Conclusions

The preliminary findings of this ongoing investigation of nine representative seam weld samples from a ~218,000 tonne order of X70 UOE pipe production, from the same project, with Ti/N ratios varying from 2.0 to 4.2 are:

1. There was no obvious effect of Ti/N ratio on the weldment microstructures or the grain size in the CGHAZ for this particular base steel composition. This is an important finding given the tendency of some specifiers to seek to limit Ti/N to hypostoichiometric values.

2. Supporting the previous conclusion is the fact that there was no correlation between reported production HAZ Charpy toughness and Ti/N ratio.

3. There was a slight increase in hardness in the internal weld metal, HAZ and base metal related to the precipitation hardening effect of the second weld pass. This observation is of no significance to the performance properties of the pipe.

Further Work

Crack Tip Opening Displacement (CTOD) tests on girth and seam welds in addition to Gleeble simulations of critical regions of weld HAZ. Detailed characterization of the microstructure and precipitation phenomena is also underway and forms a part of the future investigations.

References

1. J. Moon and C. Lee, "Behavior of (Ti, Nb)(C, N) Complex Particle During Thermomechanical Cycling in the Weld CGHAZ of a Microalloyed Steel," *Acta Materiallia*, 57 (7) (2009), 2311-2320.

2. M. F. Ashby and K. E. Easerling, "A First Report on Diagrams for Grain Growth in Welds," *Acta Metallurgica*, 30 (1982), 1969-1978.

3. Y. T. Pan and J. L. Lee, "Development of TiOx-Bearing Steels with Superior Heat-Affected Zone Toughness," *Materials and Design*, 15 (6) (1994), 331-338.

4. I. Anderson and O. Grong, "Analytical Modelling of Grain Growth in Metals and Alloys in the Presence of Growing and Dissolving Precipitates - I. Normal Grain Growth," *Acta Metallurgica et Materialia*, 43 (7) (1995), 2673-2688.

5. L. P. Zhang, C. L. Davis and M. Strangwood, "Effect of TiN Particles and Microstructure on Fracture Toughness in Simulated Heat-Affected Zones of a Structural Steel," *Metallurgical and Materials Transaction A*, 30 (8) (1999), 2089-2096.

6. B. Beidokhti, A.H. Koukabi and A. Dolati, "Effect of Titanium Addition on the Microstructure and Inclusion Formation in Submerged Arc Welded HSLA Pipeline Steel," *Journal of Materials Processing Technology*, 209 (8) (2009), 4027-4035.

7. F. J. Barbaro, private communication with author, NSW Australia.

8. K. S. Bang and H. S. Jeong, "Effect of Nitrogen Content on Simulated Heat Affected Zone Toughness of Titanium Containing Thermomechanically Controlled Rolled Steel," *Materials Science and Technology*, 18 (6) (2002), 649-654.

9. M. Doi, S. Endo and K. Osawa, "Effect of Ti Content on TiN Morphology, Microstructure and Toughness in Coarse-Grained Heat Affected Zone of Ti-Containing Steels," *Welding International*, 14 (4) (2000), 281-287.

10. W. Yan, Y. Y. Shan and K. Yang, "Effect of TiN Inclusions on the Impact Toughness of Low-Carbon Microalloyed Steels," *Metallurgical and Materials Transaction A*, 37A (2006), 2147-2158.

11. S. C. Wang, "The Effect of Titanium and Nitrogen Contents on the Microstructure and Mechanical Properties of Plain Carbon Steels," *Materials Science and Engineering A*, 145 (1991), 87-94.

12. M. Chapa, et al., "Influence of Al and Nb on Optimum Ti-N Ratio in Controlling Austenite Grain Growth at Reheating Temperatures," *The Iron and Steel Institute of Japan International*, 42 (11) (2002), 1288-1296.

13. S. F. Medina et al., "Influence of Ti and N Contents on Austenite Grain Control and Precipitate Size in Structural Steels," *The Iron and Steel Institute of Japan International*, 39 (9) (1999), 930-936.

14. I. Rak, V. Gliha and M. Kocak, "Weldability and Toughness Assessment of Ti-Microalloyed Offshore Steel," *Metallurgical and Materials Transaction A*, 26A (1997), 199-206.

15. Ø. Grong, *Metallurgical Modelling of Welding* (London, UK: Institute of Materials, 1994).

16. M. Shome, "Effect of Heat-Input on Austenite Grain Size in the Heat-Affected Zone of HSLA-100 Steel," *Materials Science and Engineering A*, 445-446 (2007), 454-460.

17. K. Easterling, *Introduction to the Physical Metallurgy of Welding* (Oxford, UK: Butterworth-Heinemann, 1992), 138-172.

18. C. Li et al., "Microstructure and Toughness of Coarse Grain Heat-Affected Zone of Domestic X70 Pipeline Steel During in-Service Welding," *Journal of Materials Science*, 46 (3) (2010), 727-733.

19. R. Laitinen, *Improvement of Weld HAZ Toughness at Low Heat Input by Controlling the Distribution of M-A Constituents* (Oulu, FI: Oulu University Press, 2006), 48-138.

20. S. Moeinifar et al., "Effect of Tandem Submerged Arc Welding Process and Parameters of Gleeble Simulator Thermal Cycles on Properties of the Intercritically Reheated Heat Affected Zone," *Materials and Design*, 32 (2) (2011), 869-876.

21. S. S. Babu, "The Mechanism of Acicular Ferrite in Weld Deposits," *Current Opinion in Solid State and Materials Science*, 8 (2004), 267-278.

22. Y. Peng, W. Chen and Z. Xu, "Study of High Toughness Ferrite Wire for Submerged Arc Welding of Pipeline Steel," *Materials characterization*, 47 (2001), 67-73.

23. M. Kuroda et al., "Nanoindentation Studies of Zirconium Hydride," *Journal of Alloy and Compounds*, 368 (2004), 211-214.

24. J. G. Garland et al., "Towards Improved Submerged Arc Weld Metal," *Metal Construction*, (1975) 275-283.